JMEPEG (2012) 21:1598–1610
DOI: 10.1007/s11665-011-0075-1

1059-9495/$19.00

Overview of Inverse Thermal Analysis of Drop-by-Drop Liquid-Metal Deposition Using Green's Functions

S.G. Lambrakos, A. Shabaev, N. Bernstein, and K.P. Cooper

(Submitted September 30, 2011)

An overview is presented of general aspects of a methodology for inverse thermal analysis of drop-by-drop liquid-metal deposition based on Green's functions. This methodology is constructed according to the general physical characteristics of rapid prototyping processes employing drop-by-drop liquid-metal deposition. This methodology represents a specific extension of a methodology using basis functions that was introduced previously for inverse analysis of welding processes, and of energy deposition in general. The formal structure of the methodology follows from a specific definition of the inverse heat transfer problem, which is well posed for inverse analysis of heat deposition processes. This definition is based on the assumption of the availability of information concerning spatially distributed boundary and constraint values. This information would be obtained in principle from both experimental measurements obtained in the laboratory, as well as numerical simulations performed using models having been constructed using basic theory.

Keywords fabricated metal, modeling processes, titanium

1. Introduction

The inverse analysis of energy deposition processes requires parametric representations that are both conveniently adjustable and physically consistent with the nature of these processes. For the inverse analysis of processes involving drop-by-drop liquid-metal deposition (Ref 1-4), where built structures can be characterized by complex shapes, as well as spatially dependent thermal diffusion, parametric representations that are conveniently adjustable are more appropriate (Ref 5, 6) for modeling, simulation, and process control. It follows that a conveniently adjustable parametric representation of processes involving drop-by-drop liquid-metal deposition can be constructed using linear combinations of basis functions. And accordingly, it follows that a relatively optimal set of basis functions for construction of such a linear combination would be the Green's functions corresponding to fundamental solutions of the equation representing the system, i.e., the convective-diffusion equation. In what follows, general aspects of a numerical methodology for inverse thermal analysis of drop-by-drop liquid-metal deposition are reviewed. In particular, the purpose of this report is to present an overview of the concepts and properties underlying the methodology for inverse thermal modeling of drop-by-drop liquid-metal deposition. This overview includes discussion of underlying properties of the methodology that should provide insight for its further development and application to progressively more complex structures fabricated by means of drop-by-drop liquid-metal deposition. This methodology is constructed according to the general physical characteristics of rapid prototyping processes employing drop-by-drop liquid-metal deposition. Formally, this methodology, introduced previously for inverse thermal analysis of welding processes and of energy deposition processes in general (Ref 7, 8), employs linear combinations of basis functions. These basis functions can be either numerical or analytical functions. The formal structure of the numerical methodology follows from a specific definition of the inverse heat transfer problem, which is well posed for inverse analysis of heat deposition processes. This definition is based on the assumption of the availability of information concerning spatially distributed boundary and constraint values. This information would be obtained in principle from both experimental measurements obtained in the laboratory, as well as numerical simulations performed using models having been constructed using basic theory.

The organization of the subject areas presented is as follows. First, a brief review is given of the inverse heat deposition problem and of its specific definition for the inverse analysis methodology whose general aspects are to be reviewed. Second, a numerical methodology for inverse thermal analysis of drop-by-drop liquid-metal deposition is described in terms of linear combinations of basis functions, according to the general physical characteristics of such processes. Third, an overview of general aspects of this numerical methodology is presented. This overview entails a discussion of the concepts and properties underlying this methodology. Fourth, a discussion concerning the interpolation property of the methodology is presented. Emphasis is given to this property in that it provides the underlying foundation for the use of approximate analytical and numerical model representations for quantitative inverse analysis. That is to say, this property provides the means for the inclusion of constraint information that in fact tends to compensate for errors associated with approximate analytical

S.G. Lambrakos, N. Bernstein, and **K.P. Cooper**, Center for Computational Materials, Code 6390, Materials Science and Technology Division, Naval Research Laboratory, Washington, DC; and **A. Shabaev**, Department of Physics, George Mason University, Fairfax, VA. Contact e-mail: lambrakos@anvil.nrl.navy.mil.

or numerical model representations. Fifth, a discussion concerning the computational complexity of Green's function-based algorithms is presented. An important aspect of algorithms based on Green' functions is that they tend have a lower computational complexity relative to algorithms based on discrete finite-difference or finite-element representations. This is shown to be the case for inverse thermal analysis of drop-by-drop liquid-metal deposition. Sixth and seventh, brief discussions are presented concerning the relationship between direct and inverse models and of path-weighted diffusivity, respectively. And finally, a conclusion is given.

2. The Inverse Heat Deposition Problem

The inverse heat transfer problem (Ref 7, 8) may be stated formally in terms of source functions (or input quantities) and multidimensional fields (output quantities). The statement of the inverse problem given here is focused on aspects of the inverse heat deposition problem related to the determination of heat fluxes via appropriate regularization of their spatial and time distributions. In general, the formulation of a heat conductive system occupying an open bounded domain Ω with an outer boundary S_o and an inner boundary S_i (see Fig. 1) involves the parabolic equation

$$\frac{\partial T(\hat{x},t)}{\partial t} + \hat{V}(\hat{x},t)\cdot\nabla T(\hat{x},t) = \nabla\cdot(\kappa(\hat{x},t)\nabla T(\hat{x},t)) + Q(\hat{x},t) \quad \text{(Eq 1a)}$$

for $T(\hat{x},t)$ in $\Omega\times(0,t_f)$, with initial condition $T(\hat{x},0)=T_a(\hat{x})$ in Ω, and Dirichlet boundary conditions on the outer and inner boundaries S_i and S_o as follows

$$T(\hat{x},t) = T_i(\hat{x}_s,t) \quad \hat{x}_s\in S_i \quad \text{(Eq 1b)}$$

on $S_i\times(0,t_f)$, and

$$T(\hat{x},t) = T_o(\hat{x}_s,t) \quad \hat{x}_s\in S_o \quad \text{(Eq 1c)}$$

on $S_o\times(0,t_f)$. Here $\hat{x}=(x,y,z)$ is the position vector, t_f is the final time, $T(\hat{x},t)$ is the temperature field variable, $\kappa(\hat{x},t)$ is the thermal diffusivity field variable, $T_a(\hat{x})$, $T_i(\hat{x},t)$, and $T_o(\hat{x},t)$ are specified functions, and $Q(\hat{x},t)$ is the volumetric heat source function. Determination of the temperature field via solution of Eq 1a to 1c defines the direct initial-boundary value problem. The inverse problem considered here is that of reconstructing the temperature field $T(\hat{x},t)$ for all time $t\in[0,t_f]$ based on available information concerning the functions defined by Eq 1b and 1c. This information must be acquired either experimentally or via direct numerical simulation.

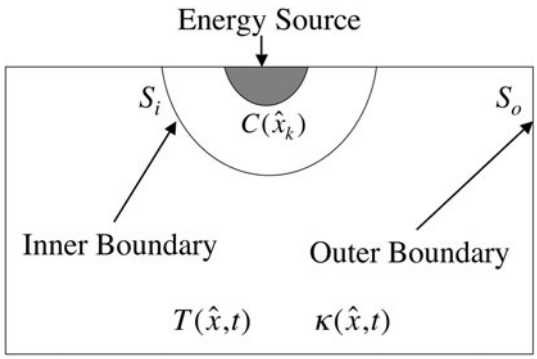

Fig. 1 Schematic representation of inner and outer boundaries of temperature field that define inverse heat deposition problem

Following the inverse analysis approach, a parametric representation based on a physical model provides a means for the inclusion of information concerning the physical characteristics of a given energy deposition process. It follows then that for heat deposition processes involving the deposition of heat within a bounded region of finite volume, consistent parametric representations of the temperature field are given by

$$T(\hat{x},t,\kappa) = T_A + \sum_{k=1}^{N_k} T_k(\hat{x},\hat{x}_k,t,\kappa) \quad \text{and} \quad T\left(\hat{x}_n^c,t_n^c,\kappa\right) = T_n^c \quad \text{(Eq 2)}$$

where the quantity T_A is the ambient temperature of the workpiece and the locations $\hat{x}_n^c$ and temperature values T_n^c specify constraint conditions on the temperature field. The functions $T_k(\hat{x},\hat{x}_k,t,\kappa)$ represent an optimal basis set of functions for given sets of boundary conditions and material properties. The quantities $\hat{x}_k=(x_k,y_k,z_k)$, $k=1,\ldots,N_k$, are the locations of the elemental source or boundary elements.

Although heat and mass deposition processes may be characterized by complex coupling between the liquid-metal drop and built structure, in terms of inverse analysis the general functional forms of the temperature fields associated with all drop-by-drop liquid-metal deposition processes are within a restricted class of functions, i.e., optimal sets of functions. Accordingly, a sufficiently optimal set of functions is that of analytic and numerical solutions to heat conduction equation for a finite set of boundary conditions (Ref 9). A parameterization based on this set is both sufficiently general and convenient relative to optimization.

The formal procedure underlying the inverse method considered here entails the adjustment of the temperature field defined over the entire spatial region of the sample volume at a given time t. This approach defines an optimization procedure where the temperature field spanning the spatial region of the sample volume is adopted as the quantity to be optimized. The constraint conditions are imposed on the temperature field spanning the bounded spatial domain of the workpiece by minimization of the value of the objective functions defined by

$$Z_T = \sum_{n=1}^{N} w_n\left(T(\hat{x}_n^c,t_n^c,\kappa) - T_n^c\right)^2 \quad \text{(Eq 3)}$$

where T_n^c is the target temperature for position $\hat{x}_n^c=\left(x_n^c,y_n^c,z_n^c\right)$.

The input of information into the inverse model defined by Eq 2 and 3 is effected by: the assignment of individual constraint values to the quantities T_n^c; the form of the basis functions adopted for parametric representation; and specifying the shapes of the inner and outer boundaries, S_i and S_o, respectively, which bound the temperature field within a specified region of the workpiece.

At this point, it is significant to note the following. First, the general trend features of heat deposition processes are such that the construction of a complete basis set of functions $T_k(\hat{x},\hat{x}_k,t,\kappa)$ making up a linear combination of the form defined by Eq 2 for representation of the associated temperature field is well defined and readily achievable. Second, for heat deposition processes, characteristics of the temperature field are poorly correlated to characteristics of the energy source. The

characteristics of the temperature field that are associated with these processes, however, are strongly coupled only to inner boundaries on this field, e.g., the solidification boundary. This property follows from the low-pass spatial filtering property of the basis functions $T_k(\hat{x}, \hat{x}_k, t, \kappa)$, whose general forms are consistent with the dominant trend features of heat deposition processes. Third, given a consistent set of basis functions, the temperature field associated with a heat deposition process is completely specified by: the shape and temperature distribution of a given inner boundary on the domain of the temperature field; the diffusivity κ, and speed of deposition V. Fourth, the shape and temperature distribution of a specified inner boundary S_i is determined by the rate of energy deposited on the surface of the workpiece and the strength of coupling of the energy source to the workpiece. And finally, in that an inner boundary S_i is defined by its shape and the distribution of temperatures on its surface $T(\hat{x}_S)$, it follows that one can define a multidimensional temperature field $T(\hat{x},\ \kappa,\ V,\ T(\hat{x}_S),\ \hat{x}_S \in S_i)$.

3. Inverse Thermal Modeling of Drop-by-Drop Liquid-Metal Deposition

As demonstrated in previous studies, the parametric representation of the form given by Eq 2 is sufficiently flexible for construction of temperature fields associated with heat deposition processes where source and workpiece characteristics are relatively simple. It is significant to note, however, that many energy deposition processes are characterized by volumetric coupling of the energy source and associated diffusion patterns that are relatively complex. Accordingly, it would be advantageous to extend the adjustability of the mapping defined by Eq 2 for the purpose of representing more complex diffusion patterns. As shown previously, the adjustability of the parameterization can be extended by adopting basis functions whose spatial distributions are spatially modulated. Among the many different possible types of spatial modulation that can be applied are those whose application produces diffusion patterns that are directionally or path weighted.

Given the parameterization framework defined by Eq 1, 2 and 3, it follows that a consistent representations, in terms of basis functions, of the temperature field associated with heat diffusion patterns are

$$T(\hat{x}, t) = T_A + \sum_{k=1}^{N_k} \sum_{n=1}^{N_t} C(\hat{x}_k) F(\hat{x}, \hat{x}_k, n\Delta t, \kappa(\hat{x})) \delta(n\Delta t - t_k) \quad \text{(Eq 4)}$$

where

$$F(\hat{x}, \hat{x}_k, t, \kappa(\hat{x})) = \frac{1}{t^{3/2}} \exp\left[-\frac{(x - x_k)^2 + (y - y_k)^2 + (z - z_k)^2}{4\kappa(\hat{x}) t} \right] \quad \text{(Eq 5)}$$

and

$$C(\hat{x}_k) = \sum_{k=1}^{N_k} q_k \delta(\hat{x} - \hat{x}_k) \delta(t - t_k) \quad \text{(Eq 6)}$$

$t = N_t \Delta t$ and $\delta(\hat{x})\delta(t)$ is the product of Dirac delta functions representing the instantaneous deposition at locations $\hat{x}_k = (x_k, y_k, z_k)$ at times $t = t_k$. It follows from Eq 5 that the speed of energy deposition V_k is an implicit function of position and is given by

$$V_k = \frac{x_k - x_{k-1}}{t_k - t_{k-1}}. \quad \text{(Eq 7)}$$

It is significant to note, and is well known, that the Green's function Eq 5 has various extensions (see Ref 9) according to different types of boundary conditions that could possibly be imposed on the built structure.

Referring to Eq 4-6, it is to be noted that spatial modulation of the diffusion field can be achieved through functional dependence on the diffusivity function $\kappa(\hat{x})$. Accordingly, the procedure for inverse analysis defined by Eq 1-6 entails adjustment of the parameters $C(\hat{x}_k)$, $\hat{x}_k$, Δt, and $\kappa(\hat{x})$ defined over the entire spatial region of the workpiece. With respect to inverse analysis, a functional form for $\kappa(\hat{x})$ can be adopted that is based on path-weighted diffusivity in order that heat diffusion be consistent with the general trend features of anisotropic diffusivity. This would be necessary for inverse thermal analysis of inhomogeneous systems. The goal of using a reasonably optimal set of basis functions for parametric representation, however, implies the necessity of adopting a form of $\kappa(\hat{x})$ that is physically consistent with heat diffusion occurring within materials having anisotropic diffusivity.

4. Concepts and Properties Underlying Inverse Thermal Modeling of Drop-by-Drop Liquid-Metal Deposition

The following concepts and properties concerning the inverse-problem approach and methodology applied to the analysis of heat deposition processes have been discussed and illustrated by various case study analyses that have been referenced in the literature and are very important for the understanding and application of the inverse-problem practices. An overview of these concepts and properties are now presented within the context of inverse thermal analysis of drop-by-drop liquid-metal deposition.

(1) The direct-problem approach to the analysis of heat deposition processes can be defined as a method in which the temperature field throughout the region of interest within the workpiece is predicted using either an explicit numerical solution of the coupled equations of energy, momentum, and mass transport or an explicit physical model based on analytical solutions to the heat conduction equation for a given set of boundary conditions. The direct-problem approach requires an a priori knowledge of the physical characteristics of the energy source and of the nature of its coupling to the workpiece. Further, this approach requires knowledge of the thermal and fluid flow properties, as a function of temperature, of the material making up the workpiece.

(2) The inverse-problem approach to the analysis of heat deposition processes can be defined as an approach in which the temperature field throughout the region of interest within the workpiece is predicted using a model representation whose form is relatively conve-

nient or optimal for adjustment of parameters. The adjustment of parameters is according to the characteristics of the experimental data concerning the actual temperature field at various locations that are sufficiently distributed spatially and temporally through the region of interest within the workpiece. The model representation adopted for an inverse-problem approach can be based on either parametric or discrete-field formulations. Parametric formulations can range from those that include detailed descriptions of the underlying physical processes to those characterized by interpolation functions whose forms are relatively simple. Discrete-field formulations consider a discrete three-dimensional field representation of the temperature field. In this type of formulation the discrete temperature field values themselves are to be adjusted according to the characteristics of the experimental data.

(3) The inverse-problem approach presented here is formally equivalent to constrained parameter optimization of the simulated temperature field using both parametric and discrete-field representations.

(4) A parametric representation based on a physical model, or direct-problem formulation, provides a means for the inclusion of information concerning the general physical characteristics of the process, which is in addition to that provided by localized constraints, and therefore provides an implicit global constraint on the parametric model representation, which is based on theory.

(5) Optimization criteria are satisfied in principle by minimization of an objective function Eq 3, which is defined in terms of experimental data concerning the temperature field and associated heat deposition process that are sufficiently distributed in space and time. In the case of processes employing drop-by-drop liquid-metal deposition this data would include the average initial temperature and location of each drop and the temperature history at sampling points measured using thermocouples.

(6) Procedures for minimization of the objective function can in principle be enhanced based on the observation that thermal profiles resulting from heat deposition processes can be represented by a relatively small class of geometric shapes.

(7) In general, information concerning material properties, fluid flow properties, and the physical character of a given heat deposition process can be represented implicitly via a specified distribution of temperature values over a closed surface bounding a given region of the workpiece.

(8) The inverse-problem approach can be extended, in principle, for the determination of quantities that can be related to material properties.

(9) The uniqueness and sensitivity of the simulated temperature field relative to parameter optimization are dominant characteristics of the inverse heat conduction problem. The inverse heat conduction problem must be well defined relative to these aspects in order that it is not ill posed. Accordingly, the inclusion of detailed information related to liquid-metal shape and temperature distribution will tend to be not relevant for determination of the temperature field characteristics outside the region of the droplet.

(10) The concept of an apparent heat source as viewed from the perspective of a specified region of interest within the temperature field represents a significant aspect of the inverse-problem approach for analysis of heat deposition processes. This concept establishes a foundation for the modeling of far-field contributions to the temperature field due to individual liquid-metal droplets.

(11) The types of experimental information that are useful for inverse thermal analysis of drop-by-drop liquid-metal deposition processes are solidification cross sections, thermocouple measurements, relative position, and spatial character of energy source, energy per deposit, liquid-drop morphology, surface features of fabricated structure, and any information related to the temperature history of the heat deposition process including transformation temperatures that can be deduced from analysis of microstructure.

(12) Inverse analyses tend to compensate for fragmented or incomplete information concerning the detailed characteristics of a given heat deposition process.

(13) Models that are structured for inverse analysis tend to be insensitive to strong nonlinearities or sharp transitions in scale.

(14) Models that are structured for inverse analysis tend to be more efficient computationally than model representations based entirely on first principles or prior knowledge, i.e., direct-problem approaches.

(15) Direct-problem formulations tend not to be "data-driven," but require that the input of information be accomplished only through the assignment of values of physical parameters. These formulations are inherently not structured for the representation of over-determined systems or systems whose characterization is in terms of large data sets.

(16) Direct-problem and inverse-problem formulations posses an interrelationship that is important with respect to analyses based on the inverse-problem approach. An aspect of this interrelationship is that all direct-problem based parametric representations may be adopted for inverse analysis, and that in general, direct-problem analyses can be interpreted as inverse-problem analyses. This interrelationship implies that a reasonable starting point for the formulation of an inverse-problem based parametric representation is to adopt a direct-problem based parametric representation as an initial ansatz for further modification (or optimization) according to the characteristics of the experimental data concerning the field quantities of interest.

(17) The general solution to an inverse problem is not a model of the system whose characteristics are considered for analysis, but rather a set of models that are consistent with both the data and a priori information concerning the system.

(18) The inverse-problem approach to the analysis of physical processes, or systems in general, has been applied to a wide range of applications. Among the many inverse problems associated with the analysis of physical systems, the inverse heat transfer problem defines a particular class of problems that are characterized by a particular range of system-response properties. Our inverse-problem approach considers a specific category of the inverse heat transfer problem, i.e., those

associated with drop-by-drop liquid-metal deposition. Further discussion concerning the inverse-problem approach in general can be found elsewhere (Ref 7, 8).

(19) *Parametric models adopted for inverse analysis can be approximations of models based on theory.* In that the calculated temperature field is adjusted according to constraint information, the parametric model representation of the temperature field can be constructed based on approximations. This follows in that the inclusion of Eq 3 provides an interesting property with respect to error propagation. Referring to Eq 3, one notes that the calculated temperature field is, at any given time, in principle, "corrected" according to values of target temperatures T_n^c. It follows that by inclusion of Eq 3, which is with respect to an inverse-problem perspective, the representation defined by Eq 2 and 3 is equipped with a predictor-corrector property for calculating the time-dependent temperature field. That is to say, any error propagation that is related to time step size, tending to cause the calculated temperature field to deviated from its correct values, is corrected for within a specified tolerance $Z_T < \varepsilon$, at those times when Eq 3 is applied and parameters are adjusted accordingly.

(20) In that the functions $T_k(\hat{x}, \hat{x}_k, t, \kappa)$ represent an optimal basis set of functions for given sets of boundary conditions and material properties, it follows that Green's functions for the heat condition equation would be a good choice.

(21) *Processes based on drop-by-drop liquid-metal deposition are characterized by multiple space and time scales.* In particular, one can associate solidification of individual liquid-metal droplets with relatively small space and time scales, while associating heat transfer to points within the built structure, from the different droplet sites, with relatively larger space and time scales. The difference in space and time scales is described schematically in Fig. 2. It is significant to note that the model representation defined by Eq 4-7 permits the embedding of fine-scale model representations that would represent the interaction of liquid-metal droplet with a built structure.

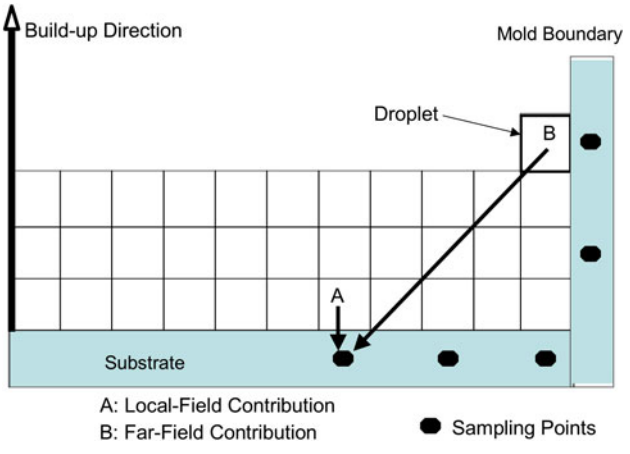

Fig. 2 Schematic representation of local and far-field contributions to a given temperature sampling point

(22) *Interpretation of parametric model in terms of numerical methods.* The parametric model representation defined by the linear combination of analytic functions given by Eq 4 through Eq 6 can be interpreted in terms of numerical methods. This follows in that each drop can be associated with a finite volume element that is active throughout the time evolution of the system. Accordingly, Eq 4-6 represent a discrete representation of drop-by-drop liquid-metal deposition, when diffusivity varies reasonably as a function of position that is unconditionally stable with respect to time step size.

(23) *The diffusivity function $\kappa(\hat{x})$ represents an adjustable quantity with respect to inverse analysis.* The parametric model representation defined by Eq 4-6, defines a diffusivity function that is inherently a time and space averaged quantity. Accordingly, only approximate values of $\kappa(\hat{x})$ are needed for inverse analysis. This characteristic of $\kappa(\hat{x})$ is consistent with the general property that parametric models adopted for inverse analysis can be approximations of models based on theory. In addition, however, this characteristic of $\kappa(\hat{x})$ implies that information concerning the diffusivity function for a given material, or combination of materials, can be deduced using inverse analysis. This interpretation of $\kappa(\hat{x})$ as a field quantity to be constructed by inverse analysis, in addition to the temperature field, is described schematically in Fig. 1.

(24) *Specification of inner and outer boundaries S_i and S_o, respectively, for drop-by-drop liquid-metal deposition.* Shown in Fig. 3 are calculations of the time-dependent temperature field (°C) of a two-dimensional built structure during formation of its fifth layer. Values of the model parameters for this calculation are given elsewhere (Ref 6). This calculation is examined with respect to the inverse analysis formalism defined above. Referring to Fig. 3, one can associate the boundary defined by the liquidus temperature (i.e., boundary between dark and light region) with an inner boundary S_i, and similarly, the temperature history at any point on the surface of the built structure with an outer boundary S_o. It is significant to note that, in principle, temperatures associated with both S_i and S_o are experimentally observable and therefore adoptable as constraints for application of the procedure defined by Eq 4-6.

5. Interpolation Property of Inverse Analysis Methodology

The specific definition of the inverse heat conduction problem given by Eq 1 implies an underlying interpolation structure whose existence should in principle provide for further extension of the methodology described above. This property, which is somewhat intuitively obvious, can be described with reference to Fig. 1. Specifically, one notes that the general parametric representation given by Eq 2, which is that of a linear combination of basis functions and constraint conditions, establishes fundamentally an interpolation between boundary values $T(\hat{x}, t) = T_i(\hat{x}_s, t)(\hat{x}_s \in S_i)$ and $T(\hat{x}, t) = T_o(\hat{x}_s, t)(\hat{x}_s \in S_o)$.

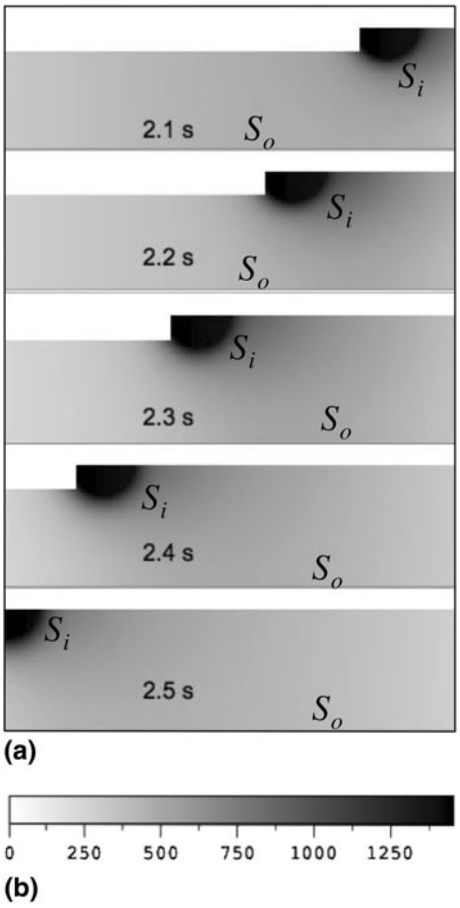

Fig. 3 (a) Specification of inner and outer surface boundaries S_i and S_o for time-dependent temperature field (°C) of two-dimensional built structure during formation of fifth layer. (b) Temperature field gray scale from 0 to 1455 °C

First, it is to be noted that given a discrete-field representation of the temperature distribution, the interpolation operator is defined by the expression

$$T_p^n = \frac{1}{6}\sum_{k=1}^{6} T_k^n, \qquad \text{(Eq 8)}$$

where the subscripts index discrete locations in space and the superscripts index sequential discrete time steps. The index k denumerates the six neighbor nodes of node p.

Next, it is interesting to note that the general form of any discrete solver for the parabolic equation Eq 1, explicit, implicit or semi-implicit (see Ref 10), is given by

$$T_p^{n+1} = \sum_{k=1}^{6} w_k^{n+1} T_k^{n+1} + \sum_{k=1}^{6} w_k^n T_k^n. \qquad \text{(Eq 9)}$$

At this stage a formal comparison of Eq 2, 8, and 9 reveals a relatively interesting property within the context of the inverse heat conduction problem defined by Eq 1. This property concerns the fact that both Eq 2 and 8, although representing different algorithms for the inclusion of a priori information concerning material properties of the system, via specification of $\kappa(\hat{x})$ in Eq 2 and the coefficients (w_k^{n+1}, w_k^n) in Eq 9, are structured for interpolation and tend toward being equivalent to Eq 9 as the influence of boundary values $T(\hat{x},t) = T_i(\hat{x}_s,t)$ $(\hat{x}_s \in S_i)$ and $T(\hat{x},t) = T_o(\hat{x}_s,t)$ $(\hat{x}_s \in S_o)$ tends to increase.

6. Computational Complexity of Green's Functions Based Algorithms

Model representations based on Green's functions of drop-by-drop liquid-metal deposition are significant in that the general complexity of an algorithm for inverse modeling of such processes can be reduced. This reduction of algorithm complexity can be shown using the mathematical formalism of algorithm complexity theory. Accordingly, the complexity of an algorithm can be expressed in terms of its computational cost N_{lbl}, which represents the number of operations required for its implementation. For the general modeling of drop-by-drop liquid-metal deposition this quantity may be decomposed into different contributions such that

$$N_{lbl} = N_d N_t N_x N_y N_z \qquad \text{(Eq 10a)}$$

where

$$N_d = N_S N_q \qquad \text{(Eq 10b)}$$

and

$$N_q = N_V N_B \qquad \text{(Eq 10c)}$$

The different factors contributing to the computational cost N_{lbl}, Eq 10a to 10c, are as follows. The quantities N_d and N_t are the number of droplets and discrete time steps, respectively, $N_x N_y N_z$ is the size of the system in terms of number of discrete volume elements, N_S and N_q are the number of elemental heat sources per droplet and the number of operations per heat source element, respectively. The number of operations N_q is in principle decomposable, i.e., Eq 10c, into the number of operations associated with volumetric heat transfer N_V and that number associated with weighting of heat transfer by the presence of nonconducting boundaries N_B. It is significant to note that the filtering properties associated with heat diffusion impose conditions such that $N_S = 1$ and that the calculation of temperature histories at a finite number of sample points provides a significant reduction in size of simulations in that essentially $N_x N_y N_z = 1$.

Referring to Fig. 2, it is to be noted that the local contribution to any given sampling point is calculated using model representations of droplet interaction with the ambient material making up the structure at that location. This contribution is assumed to occur on different space and time scales than those associated with the far-field contributions. Typically, the algorithmic complexity of any model representation of drop-structure interaction would be that characteristic of a discrete solver for the parabolic equation Eq 1, i.e., Eq 9.

7. Relationship Between Direct and Inverse Models

Strictly speaking, Eq 5 and its various extension according to different types of boundary conditions are solutions to the heat conduction equation only for the case of $\kappa(\hat{x})$ equal to a constant value. For this case the representation defined by the linear combination Eq 4-7 could be considered an approximate model representation of drop-by-drop liquid-metal deposition, which is based on the direct-problem approach, where it is assumed that the constant value of $\kappa(\hat{x})$ can be adopted as a

quantitatively accurate material property. The generalization of Eq 5 for the inclusion of a diffusivity function $\kappa(\hat{x}, t)$, which is in general not independent of position or of time, cannot be interpreted in terms of solutions to the heat conduction equation. For this case, consistent with the inverse-problem approach, the parametric model representation defined by the linear combination Eq 4-7 is to be interpreted in terms of a parameter optimization problem, i.e., parameter optimization according to minimization of a specified objective function Eq 3.

8. Path-Weighted Diffusivity

The generalization of Eq 5 for the inclusion of a diffusivity function $\kappa(\hat{x}, t)$ is based on the interpretation of the model representation Eq 4-7 in terms of a parameter optimization problem. This interpretation permits further generalization of Eq 5, and its various extensions according to different types of boundary conditions (Ref 9), for the inclusion of path-weighted diffusivity. This generalization is significant in that a path-averaged diffusivity function is consistent with the general trend features of anisotropic diffusivity. In addition, it is important to note that this generalization is to be interpreted with respect to far-field influences with respect to a given sampling point within a structure. Local influences would include spatial and temporal dependence of the diffusivity function via the form of the discrete solver for the parabolic equation Eq 1, which is adopted for modeling drop-structure interaction. With respect to far-field influences (see Fig. 2), given that a function $\kappa(\hat{x}, t)$ has been specified, a general path-dependent weighted average diffusivity can be given by

$$\langle \kappa_m(r,\theta,\phi)\rangle = \frac{1}{r}\int_0^r \kappa(r',\theta,\phi)\mathrm{d}r' = \frac{1}{r}\sum_{k=1}^{N_k}\kappa(k\Delta r,\theta,\phi)\Delta r = \frac{1}{N_k}\sum_{k=1}^{N_k}\kappa(k\Delta r,\theta,\phi). \quad \text{(Eq 11)}$$

where the cylindrical coordinates (r, θ, ϕ) specify a given path relative to the location of the source. The functionality expressed by Eq 11 provides a directional path-integral weighting of the heat diffusion pattern. This directional path-weighting, however, defines a path-integral near-neighbors problem that is associated the directional tracking of diffusivity values along any given path. Further discussion concerning path-weighted diffusivity functions is given in (Ref 5, 6).

9. Prototype Analysis 1

9.1 Temperature History Due to Metal-Droplet Distribution

In this section prototype calculations are presented that consider energy deposition within a material characterized by homogeneous and isotropic thermal diffusivity. These calculations demonstrate the functional characteristics of the far-field contributions to the temperature field, as described schematically in Fig. 2. The prototype system is that of the freeform fabrication of a two-dimensional coupon for a system whose thermal diffusivity is assumed constant. The model system consists of a sequence of layers, where each layer consists of a distribution of discrete energy sources whose strengths are assigned by the values of the coefficients $C(\hat{x}_k)$ defined in Eq 6 and are numerically integrated, or summed discretely, at each time step. Each of the discrete energy sources represents a discrete liquid-metal droplet of a given volume. The translation speed of the sample relative to the point of liquid-metal deposition is assigned implicitly through the time dependence and relative locations of the discrete energy sources, $C(\hat{x}_k)$. That is to say, a certain number of drops per layer and a certain number of layers as a function of time are specified. The model parameters used for the prototype analysis are listed in Table 1. For purposes of this analysis, the basis function $F(\hat{x}, \hat{x}_k, t, \kappa)$ given by Eq 5 is adopted for calculation of the temperature field. These functions are the solution to the heat conduction equation for a temperature independent diffusivity and non-conducting boundaries on two surfaces that are separated by a distance l, which will correspond to the width of the two-dimensional or blade-type structure to be fabricated. Accordingly, it is assumed that for this simulation there is only conduction at the substrate boundary and that the substrate consists of a metal powder composite whose thermal diffusivity is similar to that of the fabricated structure. An additional condition imposed on the model system is that of no heat transfer into the ambient environment at the edges of the structure being fabricated. This is a realistic assumption for process conditions where droplet-by-droplet deposition is adopted for fabrication of blade-type structures. A constraint condition imposed on the temperature field is that the liquid-solid interface defined by the alloy liquidus temperature is at that of the specific metal droplet at any given position within the material. Accordingly, the values assigned to the coefficients $C(\hat{x}_k)$ were such that the average temperature of each discrete droplet was within the range of liquid metal. It is significant to note that other constraint conditions, such as melt pool dimensions and measurements of temperature via thermocouples can also be adopted for assigning values to the coefficients $C(\hat{x}_k)$. In the present prototype analysis the layers are deposited one on top of the other by traversing the passes in a zig-zag fashion as shown schematically in Fig. 4. Consistent with the filter properties associated with thermal diffusion, each melt bead droplet can be represented by a cube (see Table 1). This follows in that the filtering of fine spatial structure, which is due to the Fourier transform character of Eq 4, implies that the temperature field is insensitive to details of the shape of the melt bead droplet in the case of far-field contributions to the temperature field. It is significant to note, however, that the temperature field is sensitive to the spatial distribution of droplets, i.e., the pattern for droplet deposition, and the relative proximity of boundary conditions. The prototype analysis that follows considers calculation of the temperature field at two

Table 1 Model parameters used to determine thermal fields in droplet-by-droplet deposition process

Model parameters
Material: Ti
Diffusivity: $\kappa = 8 \times 10^{-6}$ m^2/s
Time step: $\Delta t = 0.006$ s
Drop deposited every 5 time steps
19 drops per layer
Droplet energy content: $C(\hat{x}_k) = 1.5$
Droplet volume = $(\Delta l)^3$, $\Delta l = 0.4$ mm

different a sampling points within the model structure. One near a substrate boundary, and the other near a nonconducting edge boundary.

The prototype analysis is characterized by energy deposition within a material having homogeneous and isotropic thermal diffusivity. The system consists of a two-dimensional discrete distribution of Ti metal droplets having a constant average thermal diffusivity κ (see Table 1) and melt temperature T_M = 1668 °C, which is the liquidus temperature of Ti. The prototype analysis that follows consists of temperature field calculations that demonstrate the spatial and temporal characteristics of macroscopic contributions to the temperature filed, i.e., the far-field influences. Considered are calculations of temperature fields that adopt adjusted discrete spatial distributions of the effective heat source given by Eq 6 so that the calculated cross sections of the solidification boundary satisfy, in principle, experimentally observed solidification patterns or droplets of given volume whose average temperature, which is above liquidus, has been specified. The results of these calculations are shown below for the weighted sums of basis functions defined by Eq 4.

As indicated in several previous studies, an example for the potential application of the two-dimensional model adopted for prototype analysis here is shown in Fig. 5, which is that of the fabrication of a turbine blade by laser melt-deposition (Ref 9). Referring to this figure, it can be seen that the aspect ratio defined by the thickness of this structure relative to its other dimensions is such that heat transfer is essentially two-dimensional in character.

Shown in Fig. 6 and 7 is the time-dependent temperature field at different stages of the droplet-by-droplet liquid-metal deposition processes during the formation of a structure consisting of five layers according to a zig-zag sequence of metal droplet deposition (see Fig. 4). Referring to these figures, one can establish a visual correlation of the temperature history

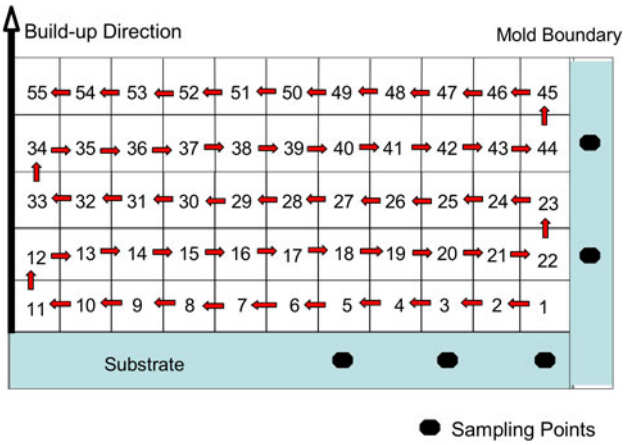

Fig. 4 Schematic representation of thermal model for inverse analysis of drop-by-drop liquid-metal deposition process

Fig. 5 A turbine blade being made by laser melt-deposition (Ref 11)

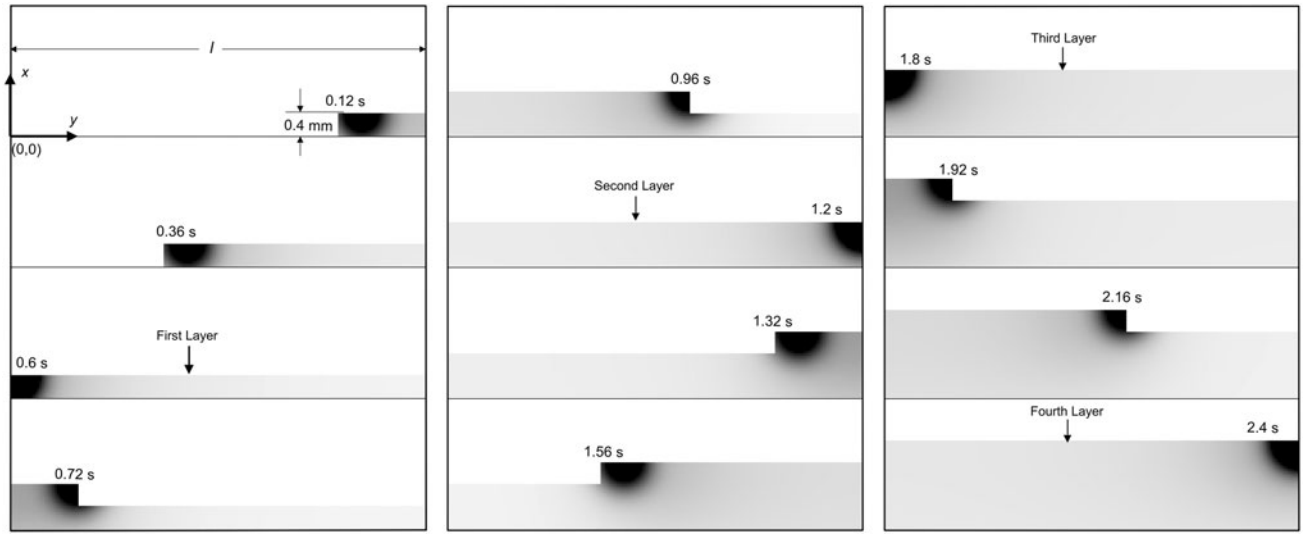

Fig. 6 Time-dependent temperature field (°C) of two-dimensional built structure according to zig-zag sequence of drop-by-drop liquid-metal deposition. Volume of each droplet is $(\Delta l)^3$, where Δl = 0.4 mm. Temperature field gray scale from 0 to 1668 °C

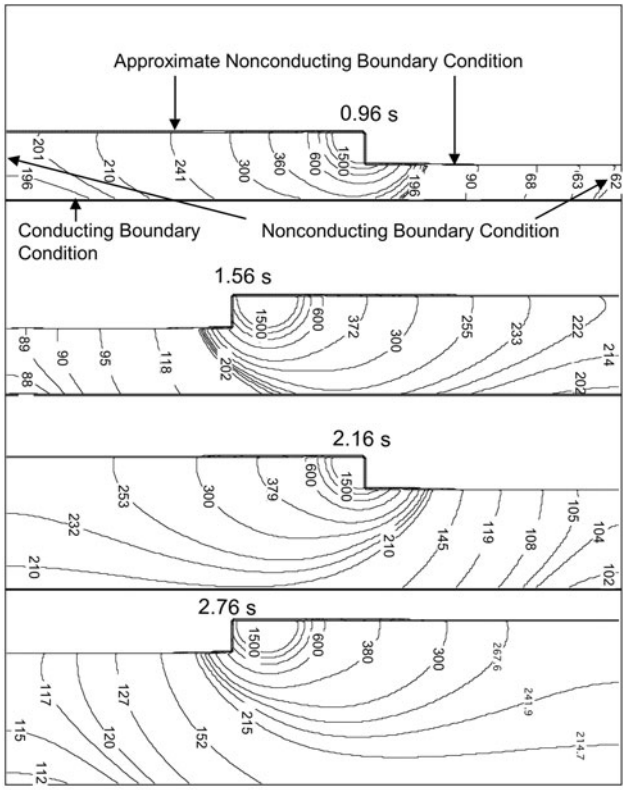

(a)

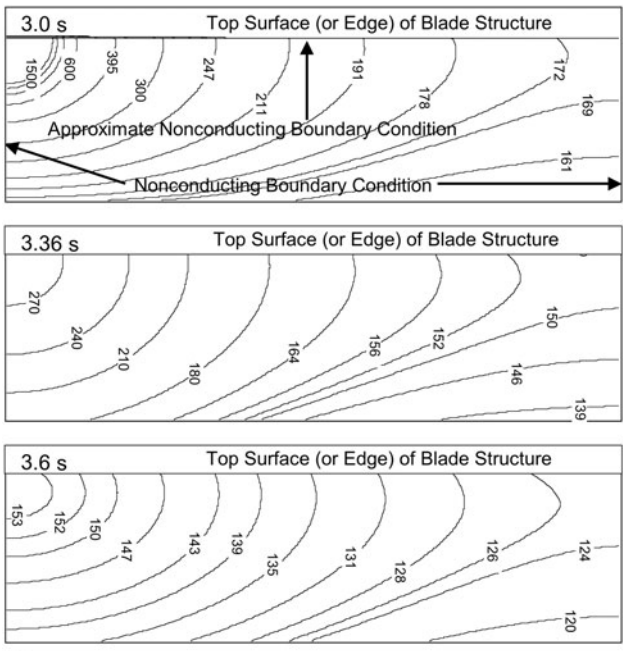

(b)

Fig. 7 (a) Time-dependent temperature field (°C) of two-dimensional built structure according to zig-zag sequence of drop-by-drop liquid-metal deposition during formation of each layer. (b) Time-dependent temperature field (°C) of two-dimensional built structure following formation of final layer

at any given sampling point with the relative position of the liquid-metal droplet at time of deposition. Accordingly, the temperature histories at any given sampling point can be examined relative to the position of the liquid-metal droplet at different stages of the droplet sequence. The results of this type of calculation are shown in Fig. 8(a) and (b).

Referring to Fig. 6, 7, and 8, and the inverse analysis formalism defined above, one can associate the boundary defined by the liquidus temperature (see Fig. 6) with an inner boundary S_i, and similarly, the temperature histories shown in Fig. 8 with a point on the surface of an outer boundary S_o. It is significant to note that, in principle, temperatures associated with both S_i and S_o are experimentally observable and therefore adoptable as constraints for application of the procedure defined by Eq 2 and 3. It is also important to note that the calculated temperatures associated with S_i can be adopted as boundary conditions for fine-scale model representations of drop-structure interaction. The type of calculating is demonstrated in the next section.

9.2 Approximate Nonconduction Boundary Conditions Using Green's Functions

At this stage it is significant to examine the application of approximate nonconduction boundary conditions using the formalism of Green's functions. These types of boundary condition are significant in that they contribute to a reduction of computational complexity of the model system, i.e., a substantial reduction of computational cost.

The nature of approximate nonconduction boundary conditions follows from the structure of the temperature fields associated with individual droplets as shown in Fig. 7(a). Referring to this figure, it is to be noted that the symmetry properties associated with a point source are equivalent to those of a nonconducting top surface boundary. One is therefore able to adopt the formalism Eq 4-6, and their various extensions (see Ref 6-8) for the representation of melt bead droplets, without the need of expending computational cost for the inclusion of top surface boundary influences. Again referring to Fig. 7(a), it can be observed that the same symmetry properties associated with a point source, which impose nonconducting boundary conditions at the surface, are extendable to a contiguous linear distribution of sources. In addition, referring to Fig. 7(a), it is observed that these symmetry properties are extendable to subsequent layers. That is to say, for each of the individual layers, the trend of the unsteady temperature field is consistent with a nonconduction top surface and windage due to the relative motion of droplet deposition and substrate. Finally, the temperature fields shown in Fig. 7(b) are examined. The temperature fields shown in this figure are for the cooling period following completion of the droplets deposition sequence. Again, it can be observed that the cooling trend is consistent with a nonconduction boundary located at the top surface of the last layer to be deposited.

10. Prototype Analysis 2

10.1 Temperature History Due to Metal-Drop-Structure Interaction

In this section prototype calculations are presented that consider energy deposition within a built structure due to individual liquid-metal droplets. These calculations demonstrate the functional characteristics of local-field contributions to the temperature field, as described schematically in Fig. 2. In

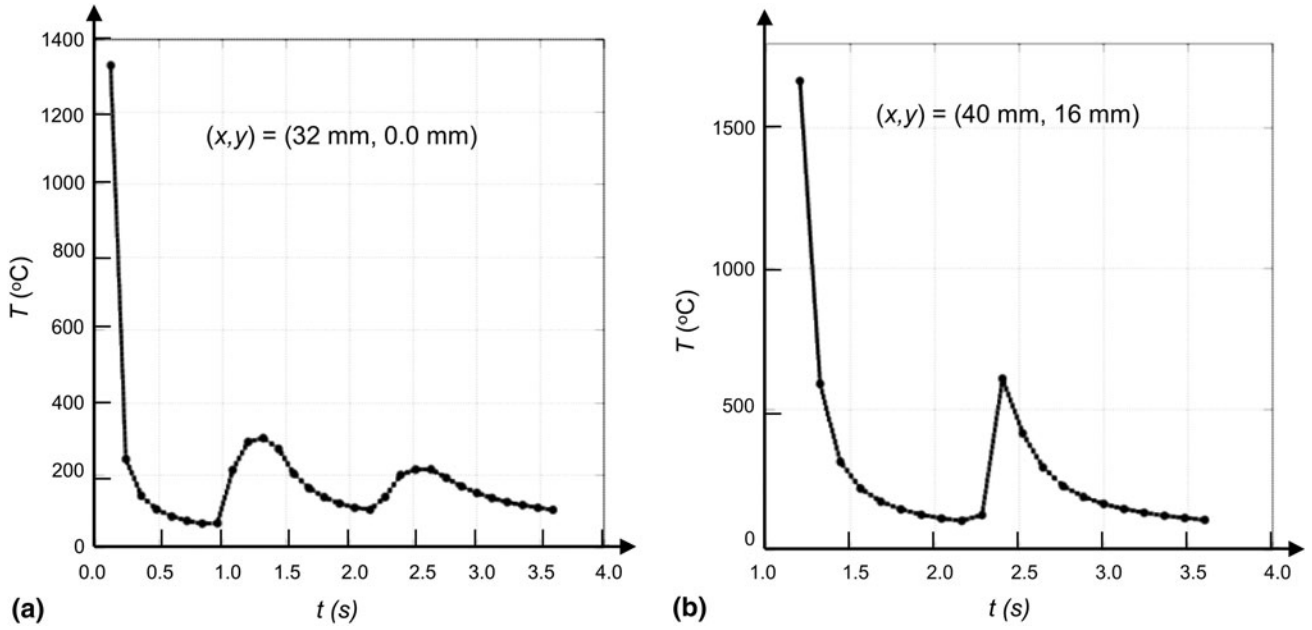

Fig. 8 Temperature histories at specific sampling points within two-dimensional built structure consisting of Ti located at (a) substrate boundary and (b) nonconducting boundary. Locations of sampling points are with respect to origin shown in Fig. 6

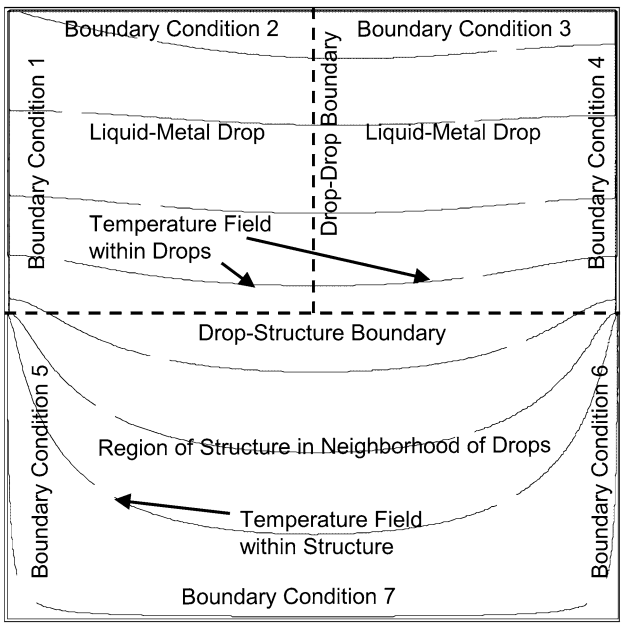

Fig. 9 Schematic representation of fine-scale model of liquid-metal-drop interaction with surface of built structure

particular, that the model representation defined by Eq 4-6 permits the embedding of fine-scale model representations (in terms of both space and time scales) that would represent the local interaction of a liquid-metal droplet with a built structure. As throughout this presentation, a quasi-two-dimensional system is considered, e.g., the system shown in Fig. 5. All discussions and associated model properties, however, are directly extendable to three-dimensional systems, e.g., built structures having shapes of coupons.

A general model for the interaction of a liquid-metal droplet with the surface of a built structure, as well as the embedding of a fine-scale model into the coarse scale model representation Eq 4-6, which is in terms of Green's functions, is shown schematically in Fig. 9. This model consists of two regions, one associated with the liquid-metal droplet and the other with the local volume of material comprising the built structure. Evolution of the temperature field resulting from interaction of these two regions is calculated using a discrete numerical solver of the form Eq 9 (see Ref 10). The boundary and initial conditions on these regions are specified according to the specific location of the liquid-metal droplet, at a given time, within or on the surface the built structure, and the local temperature field in the neighborhood of the droplet as determined by the model defined by Eq 4-6. Referring to Fig. 9, it is to be noted that information concerning the temperature, which has been calculated using the model defined by Eq 4-6, can be input to the fine-scale model via the various boundary conditions indicated. For example, for a single liquid-metal drop on the surface of the built structure, boundary conditions 1, 2, 3, and 4 would be nonconduction, while boundary conditions 5, 6, and 7 would be assigned such that the ambient temperatures near the drop-structure boundary are those determined by Eq 4-6 according to far-field influences. For this case, the initial temperature of the liquid-metal droplet would be that of the liquidus temperature of the given metal or alloy. Another example is that of an individual droplet which is adjacent to one or more other droplets at the surface of a built structure. For this case, boundary conditions 2 and 3 would be nonconduction, while boundary conditions 1 and 4 would be assigned according to temperatures of adjacent droplets, which have been calculated at previous times. Prototype calculations of temperature fields associated with deposition of liquid-metal droplets at the surface of a built structure are as follows.

The prototype analysis is characterized by energy deposition within a material having homogeneous and isotropic thermal diffusivity. The system consists of a three-dimensional liquid droplet of Ti metal having a constant average thermal diffusivity $\kappa = 5.27 \times 10^{-6} \mathrm{m}^2/\mathrm{s}$ at a melt temperature

T_M = 1668 °C, which is the liquidus temperature of Ti. Each droplet volume equals $(\Delta l)^3$, where $\Delta l = 1.0$ mm. The grid spacing and time step size adopted for application of the discrete solver, whose general form is given by Eq 9, are 0.01 mm and 2.0×10^{-6} s, respectively. The prototype analysis that follows consists of temperature field calculations that demonstrate the spatial and temporal characteristics of fine-scale contributions to the temperature field at the drop-structure boundary, i.e., local-field influences.

Shown in Fig. 10 is the time-dependent temperature field for an individual droplet at the top surface region of the built structure immediately following droplet deposition. For this prototype simulation, the boundary conditions at boundaries 1 and 2, and the drop-drop boundary, as indicated in Fig. 9, are nonconducting. In addition, for this prototype simulation, far-field boundary conditions at boundaries 5, 6, and 7, as indicated in Fig. 9, were assign values of 20 °C. This value is arbitrary and has been chosen only for the purpose of proof of concept. It is important to remember that the far-field boundary conditions 5, 6, and 7 represent adjustable quantities whose purpose is specification of a desired average temperature field within the local-field region about the drop-structure boundary. Again, this average temperature is predetermined using the Green's function formalism defined by Eq 4-6.

Shown in Fig. 11 is the time-dependent temperature field for an individual droplet, which is adjacent to a previously deposited droplet, at the top surface region of the built structure, following droplet deposition. For this prototype simulation, boundary conditions are the same as in the case of the individual droplet, except that the boundary conditions at boundaries 3 and 4, as indicated in Fig. 9, are nonconducting, and the drop-drop boundary (see Fig. 9) is made conducting. For this simulation, the temperature field within the local-field region, which includes the drop-structure boundary and drop-drop boundary will depend upon the time period between deposition of droplets according to the specific droplet deposition sequence, e.g., Fig. 4.

At this stage, it is significant to note that the fine-scale model of liquid-metal droplet deposition can be further extended in terms of inverse analysis methodology.

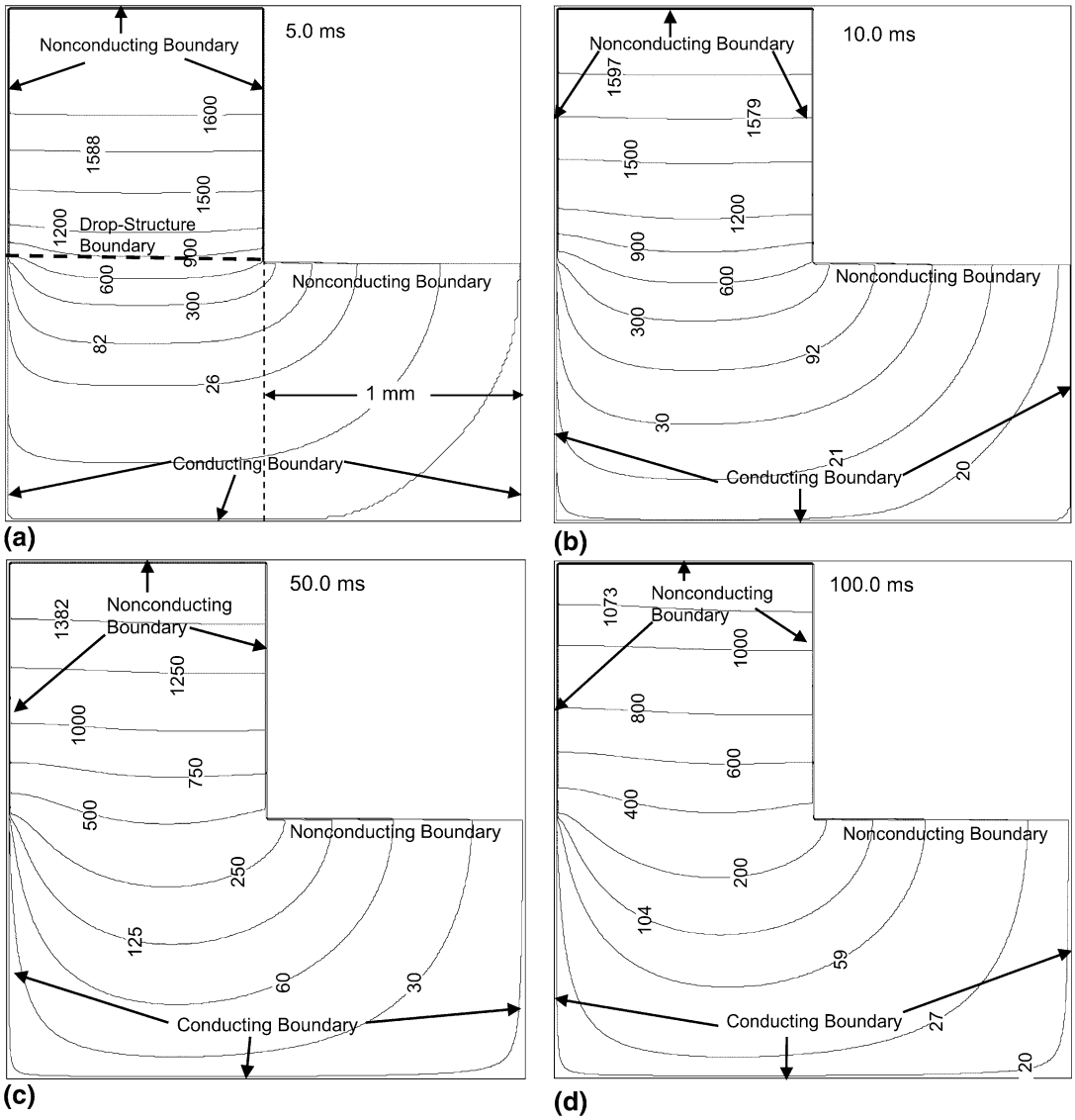

Fig. 10 Time-dependent temperature field (°C) following deposition of liquid-metal drop at surface of built structure. (a) 5.0 ms, (b) 10.0 ms, (c) 50.0 ms, (d) 100.0 ms, (e) 500.0 ms

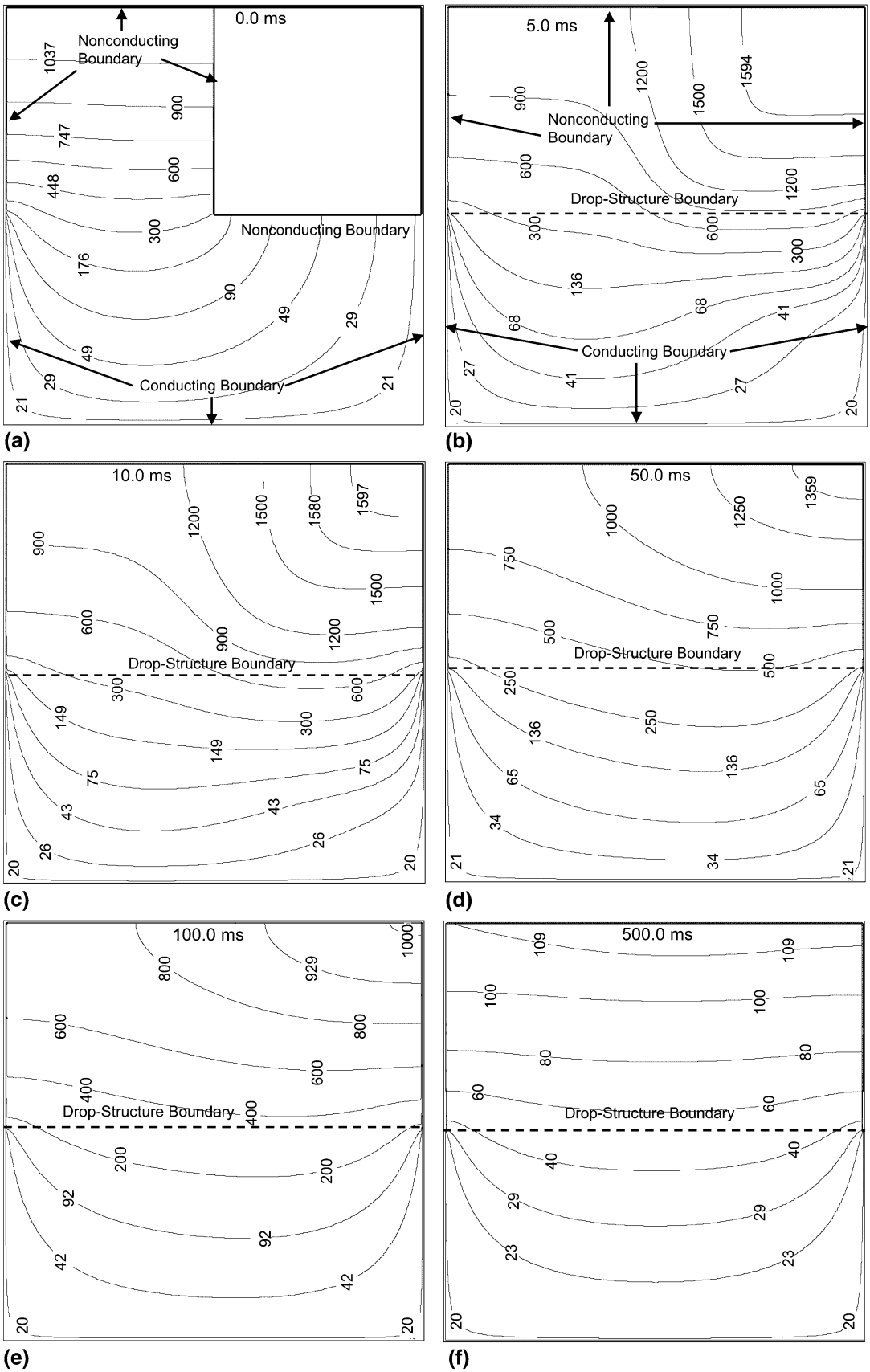

Fig. 11 Time-dependent temperature field (°C) following deposition of liquid-metal drop at surface of built structure and adjacent to previously deposited droplet. (a) 0.0 ms, (b) 5.0 ms, (c) 10.0 ms, (d) 50.0 ms, (e) 100.0 ms, (f) 500.0 ms

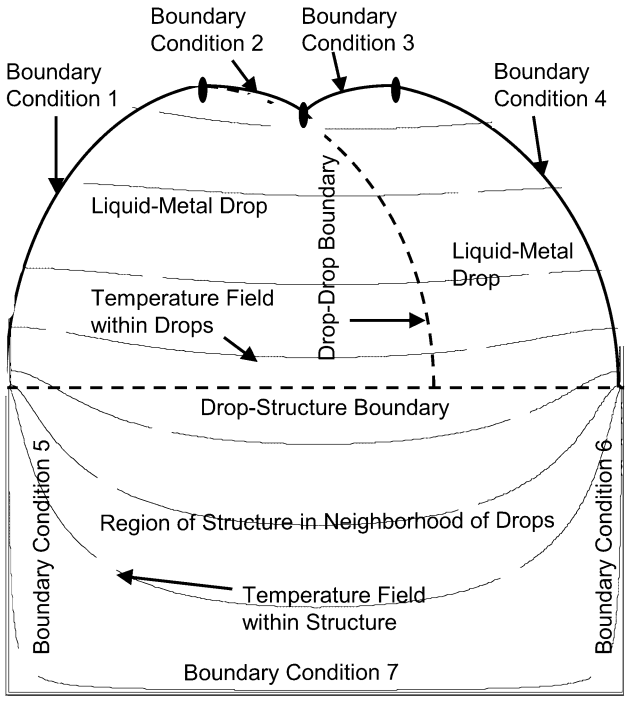

Fig. 12 Schematic representation of fine-scale model of liquid-metal-drop interaction with surface of built structure with inclusion of drop-shape information

In particular, the model representation described schematically by Fig. 9 can be extended to include droplet shape information. This type of information can be obtained either experimentally or by means of liquid-drop models for the simulation of wetting of surfaces by droplets consisting of liquids having a priori known surface tension coefficients. A schematic representation of the extension of the fine-scale model of liquid-metal droplet deposition is shown in Fig. 12. Referring to this figure, it is to be noted that the various boundary conditions are specified in terms of both conduction and shape. Consistent with the inverse modeling approach, this information is to input to the model system from available information.

11. Conclusion

The objective of this report was to present a brief overview of general aspects of inverse thermal analysis of drop-by-drop liquid-metal deposition using Green's functions, which permits the embedding of fine-scale models of liquid-metal-droplet deposition. This overview is not meant to be rigorous, but rather to provide a consolidation for convenient reference of many concepts and properties underlying inverse thermal analysis, based on Green's functions, of processes employing drop-by-drop liquid-metal deposition. Convenient reference to these concepts and properties can help to motivate further development of methods for inverse thermal analysis of such processes. Similarly, the prototype simulations presented here are for the purpose of demonstrating application of these concepts and properties for modeling drop-by-drop fabrication of realistic structures, e.g., blade structures fabricated using titanium liquid-metal droplets.

Acknowledgment

The authors thank the Office of Naval Research for its support in performing this research.

References

1. K.P. Cooper, Layered Manufacturing: Challenges and Opportunities, *Mater. Res. Soc. Symp. Proc.*, 2003, **758**, p LL1.4.1
2. G.M. Fadel and S. Morvan et al., *Solid Freeform Fabrication Proceedings*, University of Texas, Austin, TX, 2001, p 553
3. K.P. Cooper and S.G. Lambrakos, *Supplemental Proceedings, Vol. 1: Fabrication, Materials, Processing and Properties*, TMS, Warrandale, PA, 2009, p 351
4. K.P. Cooper and S.G. Lambrakos, Thermal Modeling of Direct Digital Melt-Deposition Processes, *J. Mater. Eng. Perform.*, 2011, doi:10.1007/s11665-010-9659-4
5. S.G. Lambrakos and K.P. Cooper, Path-Weighted Diffusivity Functions for Parameterization of Heat Deposition Processes, *J. Mater. Eng. Perform.*, 2011, doi:10.1007/s11665-010-9661-x
6. S.G. Lambrakos and K.P. Cooper, A Physically Consistent Path-Weighted Diffusivity Function for Modeling of Drop-by-Drop Liquid Metal Deposition, *J. Mater. Eng. Perform.*, 2011, doi:10.1007/s11665-011-9856-9
7. S.G. Lambrakos and J.G. Michopoulos, Algorithms for Inverse Analysis of Heat Deposition Processes, *Mathematical Modelling of Weld Phenomena*, Verlag der Technischen Universite Graz, Austria, Vol 8, 2007, p 847–879
8. S.G. Lambrakos and J.O. Milewski, Analysis of Welding and Heat Deposition Processes Using an Inverse-Problem Approach, *Mathematical Modelling of Weld Phenomena*, Verlag der Technischen Universite Graz, Austria, Vol 7, 2005, p 1025–1055
9. H.S. Carslaw and J.C. Jaegar, *Conduction of Heat in Solids*, 2nd ed., Clarendon Press, Oxford, 1959, p 374
10. S.V. Patankar, *Numerical Heat Transfer and Fluid Flow*, Hemisphere Publishing, New York, 1980
11. Sandia National Laboratories, *Advanced Metallurgy*, 2007, https://share.sandia.gov/8700/projects/content.php?cid=50